Intramolecular Regulation of Protein Tyrosine Phosphatase SH-PTP1: A New Function for Src Homology 2 Domains†

Dehua Pei,‡ Ulrike Lorenz,§ Ursula Klingmüller,|| Benjamin G. Neel,§ and Christopher T. Walsh*,‡

Department of Biological Chemistry and Molecular Pharmacology, Harvard Medical School, 240 Longwood Avenue, Boston, Massachusetts 02115, Molecular Medicine Unit, Beth Israel Hospital, Boston, Massachusetts 02215, and Whitehead Institute for Biomedical Research, 9 Cambridge Center, Cambridge, Massachusetts 02142

Received September 23, 1994⊗

ABSTRACT: The steady-state kinetic properties of SH-PTP1 (PTP1C, SHP, HCP), a Src homology 2 (SH2) domain-containing protein tyrosine phosphatase (PTPase), were assessed and compared with those of three truncation mutants, using *p*-nitrophenyl phosphate, phosphotyrosyl (pY) peptides, and reduced, carboxyamido-methylated, maleylated, and tyrosyl-phosphorylated lysozyme as substrates. At physiological pH (7.4), truncation of the two N-terminal SH2 domains [SH-PTP1(ΔSH2)] or the last 35 amino acids of the C-terminus [SH-PTP1(ΔC35)] activated the phosphatase activity by 30-fold and 20−34-fold relative to the wild-type enzyme, respectively. Truncation of the last 60 amino acids resulted in a mutant [SH-PTP1(ΔC60)] with wild-type activity. SH-PTP1 and SH-PTP1(ΔC60) displayed apparent saturation kinetics toward pNPP only at acidic pH (pH ≤ 5.4); as pH increased above 5.5, their apparent K_M values increased dramatically. In contrast, SH-PTP1(ΔSH2) obeyed normal Michaelis−Menten kinetics at all pH values tested (pH 5.1−7.4) with a constant K_M (10−14 mM). Furthermore, two synthetic pY peptides corresponding to known and potential phosphorylation sites on the erythropoietin (EPOR pY429) and interleukin-3 (IL-3R pY628) receptors bound specifically to the N-terminal SH2 domain of SH-PTP1 (K_D = 1.8−10 μM) and activated the catalytic activity of SH-PTP1 and SH-PTP1(ΔC60) but not SH-PTP1(ΔSH2), in a concentration-dependent manner. Maximal activation (25−30-fold) of SH-PTP1 was achieved at 70 μM EPOR pY429, and the maximally activated enzyme approached the activity of SH-PTP1(ΔSH2). Addition of EPOR pY429 peptide, which corresponds to the recently identified *in vivo* binding site for SH-PTP1, at 40 μM also completely restored the saturation kinetic behavior of SH-PTP1 (at pH 7.4) toward pNPP, with catalytic parameters (K_M = 12.8 mM, k_{cat} = 3.2 s^{-1}) similar to those of SH-PTP1(ΔSH2). These data suggest that the SH2 domains of SH-PTP1 serve to autoinhibit the phosphatase activity of the PTPase domain. A model is proposed in which the SH2 domains interact with the PTPase domain in a pY-independent fashion and drive the PTPase domain into an inactive conformation.

Transient phosphorylation of proteins on tyrosine residues represents one of the most important posttranslational modifications, playing a central role in many cellular processes such as transmembrane signaling through receptor tyrosine kinases. The levels of tyrosine phosphorylation, and thus the strength and duration of the signals transmitted, are regulated by the opposing actions of protein tyrosine kinases (PTK)[1] and protein tyrosine phosphatases (PTPases). Protein tyrosine phosphatases are, in general, much more active enzymes when compared with their kinase counterparts, implying that PTPases must function *in vivo* in a regulated fashion (Fischer et al., 1991). However, to date, little is still known about the regulation of PTPases.

Following activation of receptor PTKs, different phosphotyrosine (pY) residues on the autophosphorylated receptors recruit specific partner proteins (Koch et al., 1991) via high-affinity interaction(s) of the phosphotyrosine and the side chains of adjacent residues with the Src homology 2 (SH2) domains of the partners (Songyang et al., 1993; Waksman et al., 1993; Eck et al., 1993). A particularly intriguing class of signaling molecules are the PTKs and PTPases that contain SH2 domains. These molecules could be recruited to new pY loci and then catalytically amplify or terminate the pY-mediated signaling pathways. Although

† This work was supported by a fund from Hoffmann-LaRoche Institute for Chemistry and Medicine and grants from the National Institutes of Health (GM20011 to C.T.W., CA49152 to B.G.N., and PO1 HL32262 to H. F. Lodish) and Arris Pharmaceutical Corp. (to H. F. Lodish). D.P. was supported by a postdoctoral fellowship from the Damon Runyon-Walter Winchell Cancer Research Fund (DRG-1172), U.L. was supported by a fellowship from the American Cancer Society, Massachusetts Division, and U.K. was supported by a fellowship from Deutsche Forschungsgesellschaft. B.G.N. is the recipient of a Junior Faculty Research Award from the American Cancer Society and the Gertrude Elion Award from the American Association of Cancer Research, funded by Burroughs-Wellcome Corp.

* To whom correspondence should be addressed.
‡ Harvard Medical School.
§ Beth Israel Hospital.
|| Whitehead Institute for Biomedical Research.

⊗ Abstract published in *Advance ACS Abstracts,* December 1, 1994.

[1] Abbreviations: PTK, protein tyrosine kinase; PTPase, protein tyrosine phosphatase; SH2, Src homology 2; PDGF, platelet-derived growth factor; PDGFR, platelet-derived growth factor receptor, EGF, epidermal growth factor; EGFR, epidermal growth factor receptor; EPO, erythropoietin; EPOR, erythropoietin receptor; CSF1, colony-stimulating factor 1; CSF1R, colony-stimulating factor 1 receptor; IL-3, interleukin-3; IL-3R, interleukin-3 receptor; MBP, maltose-binding protein; pY, phosphotyrosine; pNPP, *p*-nitrophenyl phosphate; RCM-lysozyme, reduced, carboxyamido-methylated, and maleylated lysozyme; Hepes, *N*-(2-hydroxyethyl)piperazine-*N*′-(2-ethanesulfonic acid); bis-Tris, [bis-(2-hydroxyethyl)imino]tris(hydroxymethyl)methane; bis-Tris-propane, 1,3-bis[[tris(hydroxymethyl)methyl]imino]propane.

0006-2960/94/0433-15483$04.50/0

SH2-containing PTKs, e.g., the Src family, have been extensively characterized, only recently have SH2-containing PTPases been identified and initial functional analyses conducted. The new subfamily of cytoplasmic PTPases includes SH-PTP1 (Plutzky et al., 1992) [also known as PTP1C (Shen et al., 1991), HCP (Yi et al., 1992), and SHP (Matthews et al., 1992)], SH-PTP2 (Freeman et al., 1992) [also known as Syp (Feng et al., 1993), PTP1D (Vogel et al., 1993), and PTP2C (Ahmad et al., 1993)], and the *Drosophila* homolog of SH-PTP2, the *corkscrew* gene product (Perkins et al., 1992). These molecules each contain two SH2 domains N-terminal to their PTPase domain. SH-PTP1 is predominantly expressed in cells of hematopoietic origin, whereas SH-PTP2 and *corkscrew* are more ubiquitously expressed.

In order to assess the roles of the SH2 domains on specificity and catalytic activity of the SH-PTPs and to understand their functions in signal transduction, we have previously overexpressed and purified from *Escherichia coli* both SH-PTP1 (Pei et al., 1993) and SH-PTP2 (Sugimoto et al., 1993) in full-length and truncated forms. Both SH-PTPs show some unusual regulatory features. Firstly, neither enzyme displays normal Michaelis−Menten kinetics toward synthetic pY peptide substrates. Secondly, SH-PTP2 has previously been shown to be recruited to the autophosphorylated PDGF receptor (Lechleider et al., 1993a), EGF receptor (Vogel et al., 1993; Feng et al., 1993; Lechleider et al., 1993a), and insulin receptor substrate 1 (IRS-1) (Kuhne et al., 1993). The association is mediated by specific interactions of the N-terminal SH2 domain of SH-PTP2 with PDGFR pY1009 (Kazlauskas et al., 1993; Lechleider et al., 1993b), IRS-1 pY1172 (Sun et al., 1993) and an unidentified pY site(s) on EGFR. We have found that engagement by PDGFR pY1009 or IRS-1 pY1172 peptide allosterically activates the phosphatase activity of recombinant SH-PTP2 some 10−50-fold (Lechleider et al., 1993; Sugimoto et al., 1994). Recently, SH-PTP1 has been reported to bind to activated c-Kit (Yi & Ihle, 1993) and the interleukin-3 (IL-3) receptor β chain (Yi et al., 1993) in myeloid cells. We have found that SH-PTP1 binds to phosphorylated erythropoietin (EPO) receptor in EPO-dependent BaF3 cells expressing the EPO receptor (EPOR) and have mapped the binding site to pY429 on the receptor (U.K., U.L., L. C. Cantley, B.G.N., and H. F. Lodish, to be published elsewhere). Therefore, SH-PTP1 has been hypothesized to be a key regulatory element in the pY-mediated signaling that occurs in myeloid cells via IL-3 and in erythroid cells via EPO by similar recruitment to pY sites on the cytoplasmic domain of these growth factor receptors.

In this work we show that a specific pY sequence from the EPO receptor is a ligand for the N-terminal SH2 domain of SH-PTP1. Moreover, occupancy of the SH2 domain(s) relieves an inhibitory interaction between the SH2 domains and the PTPase domain of SH-PTP1, leading to a substantial increase in the catalytic efficiency of the PTPase domain. Binding of the EPO receptor peptide to the SH2 domain(s) dramatically lowers the K_M for *p*-nitrophenyl phosphate and brings the k_{cat}/K_M into the range observed with the isolated PTPase catalytic domain, consistent with physical disengagement of the SH2 domain(s) from inhibitory interaction with the catalytic domain. Thus, both SH-PTP1 and SH-PTP2 undergo marked catalytic activation upon pY ligand binding to their SH2 domains, coupling pY protein substrate recruitment to enhancement of PTPase activity and dephosphorylation of pY residues in that microenvironment.

EXPERIMENTAL PROCEDURES

Materials. All Fmoc-protected amino acids, [(benzotriazol-1-yl)oxy]tris(dimethylamino)phosphonium hexafluorophosphate (BOP), 2-(1*H*-benzotriazol-1-yl)-1,1,3,3-tetramethyluronium hexafluorophosphate (HBTU), and 1-hydroxybenzotriazole (HOBT) were purchased from Peninsula Laboratories. HMP resin was from Milligen Biosearch, and Fmoc-Tyr(PO_3Me_2)-OH was from Bachem Bioscience. *p*-Cyanophenyl phosphate (pCNPP), *p*-fluorophenyl phosphate (pFPP), *m*-chlorophenyl phosphate (mClPP), and phenyl phosphate (PP) were synthesized in this laboratory by T. J. Wandless and M. Lamarche. Other reagents were from Sigma or Aldrich.

Buffers. The following buffers were used, buffer A, 100 mM Hepes, pH 7.4, 150 mM NaCl, 1 mM EDTA, 1 mM β-mercaptoethanol (BME); buffer B (10 mM Hepes, pH 7.4, 150 mM NaCl, 3.4 mM EDTA; buffer C, 100 mM NaOAc, pH 5.1, 150 mM NaCl, 1 mM EDTA, 1 mM BME; buffer D, same as buffer C but at pH 5.4; buffer E, 100 mM bis-Tris, pH 5.7, 150 mM NaCl, 1 mM EDTA, 1 mM BME; buffer F, same as buffer E but at pH 5.8; buffer G, same as buffer E but at pH 6.3; buffer H, 100 mM bis-Tris-propane, pH 7.0, 150 mM NaCl, 1 mM EDTA, 1 mM BME.

Bacterial Protein Expression and Purification. Human SH-PTP1 (amino acids 1−595), SH-PTP1(ΔSH2) (amino cids 205−595), SH-PTP1(ΔC35) (amino acids 1−560), and SH-PTP1(ΔC60) (amino acids 1−535) were expressed in *E. coli* using the pET expression vector system and purified to homogeneity as previously described (Pei et al., 1993; Lorenz et al., 1994). Plasmid pET-SHPTP1(His•tag), in which a histidine tag (MGSSHHHHHHSSGLVPRGSH) was added to the N-terminus of SH-PTP1, was generated by replacing the 900-base pair *Nde*I-*Mlu*I fragment of pET-SHPTP1 (Pei et al., 1993) with the corresponding fragment from pET-15b (Novagen, WI). The N-terminal SH2 domain and the N+C-terminal SH2 domains were expressed as fusion proteins with maltose-binding protein (MBP). For the N-terminal SH2 domain, the *Nde*I-*Hin*dIII fragment encoding the entire SH-PTP1 was transferred from pGEX-SHPTP1 (Pei et al., 1993) into the *Nde*I-*Hin*dIII-linearized plasmid pMAL-LIM, which has been modified by inserting an *Nde*I sequence directly next to the unique *Bam*HI site (M. Li and C.T.W., unpublished results). The resulting plasmid, pMAL-SHPTP1, was then digested with *Kpn*I and *Hin*dIII, and the termini were filled in using T4 DNA polymerase. Recircularization of the larger fragment generated plasmid pMAL-SH2(N), in which the N-terminal SH2 domain was fused in-frame with the MBP coding sequence and a stop codon was placed after the arginine residue at position 109. For the N+C-terminal SH2 domain construct, plasmid pGEX-SHPTP1 was partially digested with *Bsm*I and the linearized full-length DNA was isolated and treated with T4 DNA polymerase. Circularization of this DNA generated pGEX-SH2(N+C), in which a codon for glycine was created after the asparagine residue at position 219 followed by a newly generated stop codon. Plasmid pMAL-SH2(N+C) was then generated by replacing the 1.7-kb-*Kpn*I-*Avr*II fragment of pMAL-SHPTP1 with the corresponding fragment of pGEX-SH2(N+C). pET-SH2(N+C), which encodes the N- and C-terminal SH2 domains in a nonfusion form, was constructed by replacing the 2.0-kb *Nde*I-*Sal*I

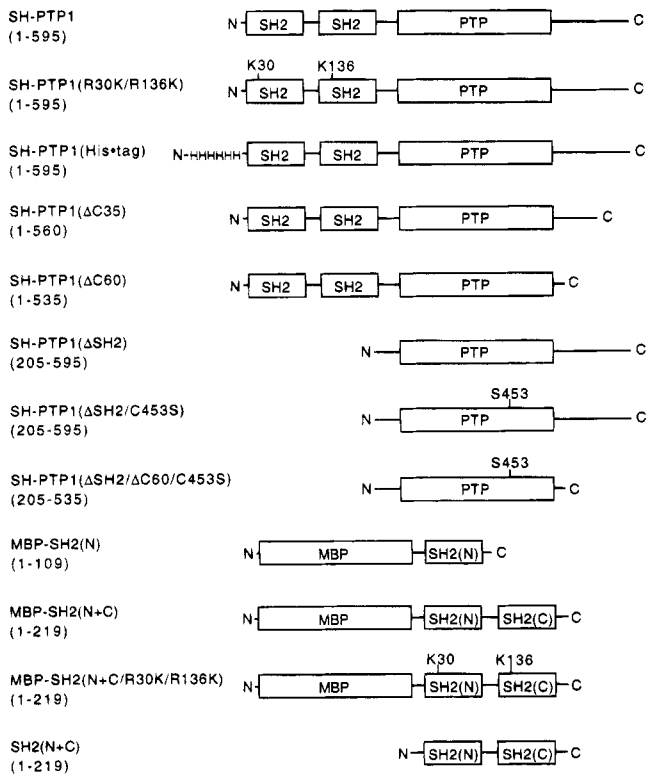

FIGURE 1: Diagram illustrating the structures of constructs used in this work. The numbers of parentheses indicate the starting and ending points within the SH-PTP1 protein used for each construct, according to the numbering scheme of Plutzky et al. (1992).

fragment of pET-SHPTP1 with the corresponding 2.0-kb *Nde*I-*Sal*I fragment from pMAL-SH2(N+C). R30K, R136K, and C453S mutations were performed with oligonucleotide primers using the method of Kunkel (1985). All mutations were verified by dideoxy sequencing. pET-SHPTP1(ΔSH2/ΔC60/C453S) was then constructed from pET-SHPTP1-(ΔSH2/C453S) in a similar fashion to that described for pET-SHPTP1(ΔC60) (Lorenz et al., 1994). Figure 1 shows a schematic representation of these constructs.

E. coli strain BL21(DE3) or DH5α transformed with the appropriate plasmids was grown, induced, and lysed, and the fusion proteins were purified on an amylose column (New England Biolabs, MA) as described (Riggs, 1990). SH-PTP1(His•tag) and SH-PTP1 (R30K/R136K) were purified by the same procedure as described for SH-PTP1 (Pei et al., 1993). The ΔSH2/C453S and ΔSH2/ΔC60/C453S mutants were purified as described for SH-PTP1(ΔSH2) (Pei et al., 1993). The isolated SH2(N+C) domains were purified by 35−60% $(NH_4)_2SO_4$ fractionation, gel filtration on a Sephacryl S-300 column, and affinity chromatography on a phosphotyrosine-Affi-Gel column. Whenever possible, freshly purified proteins were used in binding studies and enzyme assays. The rest of the purified proteins were stored at −80 °C either in the presence or absence of 33% glycerol. Protein concentrations were determined according to Bradford (1976) using bovine serum albumin (Bio-Rad) as standard.

Synthesis of Phosphotyrosyl Peptides. All phosphorylated and nonphosphorylated peptides were prepared by solid-phase synthesis using HMP resin and FMOC/BOP or HBTU/HOBT chemistry on a 0.15-mmol scale with a Milligen 504 shaker, as previously described (Cho et al., 1991). Reactions were monitored by ninhydrin analysis, and the coupling procedure was repeated once when necessary. Deprotection of phosphorylated peptides was typically carried out in two steps. The first step employed a mixture of trifluoroacetic acid (TFA; 4.5 mL), thioanisole (0.25 mL), anisole (0.1 mL), and ethanedithiol (0.15 mL) for 1 h at room temperature. The solvents were removed by a gentle flow of N_2. The peptides were then triturated and washed with diethyl ether. After drying in air, the peptides were subjected to a second deprotection step using a mixture of trimethylsilyl bromide (0.4 mL), thioanisole (0.35 mL), and *m*-cresol (0.05 mL) in TFA (2.2 mL) for 20 h at 4 °C (Kitas et al., 1989). The resulting crude peptides were purified by reverse-phase HPLC chromatography (Cho et al., 1991), and their identity was confirmed by laser desorption mass spectrometry.

Equilibrium Binding Studies. Immobilization of peptides onto Pharmacia BIAcore CM5 sensorchips was carried out as described (Felder et al., 1993). Usually, a lysine was added to the N- or C-termini of the peptides to insure adequate coupling. The density of the phosphopeptides on the surface was monitored by anti-pY antibody 4G10 (kindly provided by Brian Druker and Tom Roberts, Dana-Farber Cancer Institute). A flow of 4G10 (50 μg/mL) for 10 min at 5 μL/min usually gave approximately 2000 response units (RU). Binding experiments were conducted in buffer B (10 mM Hepes, pH 7.4, 150 mM NaCl, 3.4 mM EDTA). The equilibrium response units (R_{eq}) at each MBP-SH2 concentration were analyzed according to the equation (*Pharmacia BIAcore Mannual*, 1991):

$$R_{eq}/[SH2] = R_{max}/K_D - R_{eq}/K_D$$

where R_{max} is the maximum response at saturated binding, K_D is the equilibrium dissociation constant, and [SH2] is the concentration of MBP-SH2 protein injected.

PTPase Assay. Assays for PTPase activity using pNPP or pY peptides have previously been described (Pei et al., 1993). All pNPP and pY peptide stock solutions were adjusted to the pH values of the corresponding assay buffers prior to use except for the EpoR peptide (Ac-PHLKpY-LYLVVSDK), which was prepared as a 2 mM solution in H_2O containing 0.05% trifluoroacetic acid. The concentrations of pNPP and pY peptide solutions were determined by measuring the released *p*-nitrophenolate and inorganic phosphate, respectively, after complete hydrolysis with SH-PTP1(ΔSH2) (Pei et al., 1993). The dephosphorylation of ^{32}P-labeled RCM-lysozyme was carried out in buffer A as described (Sugimoto et al., 1993).

Activation of SH-PTP1 and mutants by pY peptides was typically carried out in 50-μL reaction mixtures containing the appropriate buffers (pH 5.1−7.4), 150 mM NaCl, 1 mM EDTA, 1 mM BME, 10 mM pNPP, 0−300 μM pY peptides, and 15−75 nM PTPase. After 30 min at room temperature, the reactions were quenched with 950 μL of 1 N NaOH, and the absorbance at 405 nm was measured. In most cases the substrate to product conversion was <10%.

RESULTS

Activation of SH-PTP1 by N-Terminal or C-Terminal Truncation. During our initial characterization of SH-PTP1, we found that, even at its optimal pH (5.5), it is much less efficient (k_{cat}/K_M on the order of 10^3 M^{-1} s^{-1}) than other PTPases, such as LAR, CD45, and human PTPβ (k_{cat}/K_M on the order of 10^5-10^6 M^{-1} s^{-1}) (Pei et al., 1993). At physiological pH (7.4), SH-PTP1 has very little activity. We envisioned that the noncatalytic domains of SH-PTP1, namely the two N-terminal SH2 domains and the extended

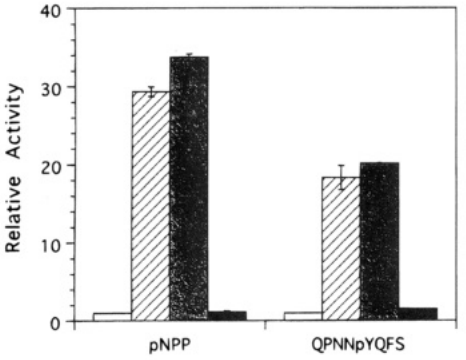

FIGURE 2: Comparison of the relative rates of full-length SH-PTP1 (open bars) and three deletion mutants, ΔSH2 (hatched bars), ΔC35 (shaded bars), and ΔC60 (closed bars), for dephosphorylating pNPP and peptide QPNNpYQFS derived from CSF1R. Reactions were carried out in buffer A (pH 7.4) as described (Pei et al., 1993), using 10 mM pNPP as substrate. The initial rates are normalized on a molar basis relative to wild-type SH-PTP1. Data presented are the mean ± SD values of three to four parallel experiments.

C-terminus, might serve as autoinhibitory elements for the catalytic domain. To test this hypothesis, we constructed three deletion mutants of SH-PTP1 (Figure 1). One mutant, SH-PTP1(ΔSH2), contains the entire PTPase domain and the C-terminus but lacks the two N-terminal SH2 domains. The second mutant, designated as SH-PTP1(ΔC35), contains both SH2 domains and the catalytic domain but lacks the last 35 amino acids of the C-terminus. The third mutant [SH-PTP1(ΔC60)] lacks the last 60 amino acids of SH-PTP1. All of these mutants were expressed in *E. coli* and purified to homogeneity.

The catalytic activities of the recombinant SH-PTP1 and deletion mutants were measured with pNPP (10 mM) as substrate in buffer A (pH 7.4). Truncation of the two SH2 domains results in 30-fold activation compared to the wild-type enzyme (Figure 2). SH-PTP1(ΔC35), which lacks part of the C-terminus, also shows a 34-fold increase in activity relative to wild-type SH-PTP1. However, truncation of the entire C-terminal domain renders SH-PTP1(ΔC60) much like wild-type SH-PTP1 (see below), with essentially the same catalytic activity. Similar increases in activity were also observed when either a synthetic phosphotyrosyl peptide (pY969 QPNNpYQFS at 500 μM) (Figure 2) derived from CSF1 receptor (Coussens et al., 1986) or ^{32}P-labeled RCM-lysozyme was used as substrate (data not shown). These results indicate that the SH2 domains are autoinhibitory. Under certain *in vitro* conditions, the C-terminus can also modulate the PTPase activity. Whether this *in vitro* effect is of physiological relevance remains to be established (see Discussion).

Differential Kinetic Behavior of SH-PTP1 and Deletion Mutants. We have previously shown that SH-PTP1 and SH-PTP1(ΔSH2) display distinct pH dependencies in their activity; while SH-PTP1 is most active at pH 5.5, SH-PTP1-(ΔSH2) is most active at pH 6.3 (Pei et al., 1993). Moreover, SH-PTP1(ΔSH2) has an apparent K_M of 24−38 mM with pNPP as substrate (at pH 6.3), whereas SH-PTP1 has a much higher apparent K_M value of 148 mM (at pH 5.5). To determine whether this 4−6-fold difference in K_M values was due to the pH difference of the assay buffers (pH 6.3 vs 5.5), we carried out kinetic analysis of SH-PTP1 and SH-PTP1(ΔSH2) at pH values ranging from 5.1 to 7.4 using pNPP as substrate. Under all conditions tested (including pH 5.1, 6.3, and 7.4), SH-PTP1(ΔSH2) displays Michaelis−

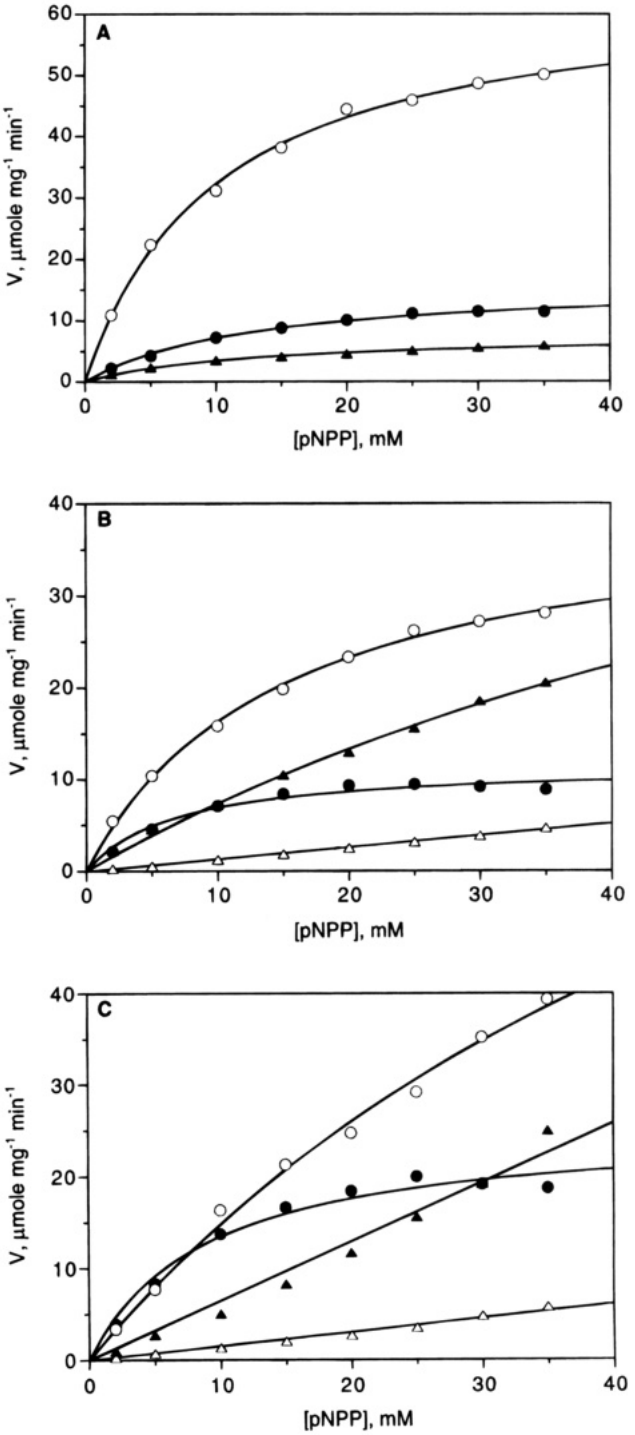

FIGURE 3: Velocity vs substrate curves for the dephosphorylation of pNPP. Experiments were carried out at indicated pNPP concentrations and pH values, and the initial rates are presented. The curves were fitted to the data according to the equation: $V = V_{max}[S]/(K_M + [S])$. For SH-PTP1(ΔSH2) (panel A), experiments were conducted at pH 5.1 (closed circles), pH 6.3 (open circles), and pH 7.4 (triangles). For SH-PTP1 (panel B) and SH-PTP1-(ΔC60) (panel C), experiments were conducted at pH 5.1 (closed circles), pH 5.4 (open circles), pH 5.7 (closed triangles), and pH 6.5 (open triangles). The buffers used were described under Experimental Procedures. Multiple experiments were carried out at each pH value, yielding similar results. Data from a typical experiment are presented.

Menten kinetics (Figure 3A). Its k_{cat} varies considerably with pH; it increases from 12.2 s^{-1} at pH 5.1 to 48.6 s^{-1} at pH 6.3 and then decreases to 5.7 s^{-1} at pH 7.4. In contrast, its K_M value remains relatively constant at 10−14 mM over this pH range. These K_M values are 2-fold lower than what we

reported previously (24−38 mM at pH 6.3). This minor discrepancy in K_M values is most likely due to the use of 2-(*N*-morpholino)ethanesulfonic acid (Mes) in our early work. We have subsequently found that Mes inhibits SH-PTP1.

Interestingly, wild-type SH-PTP1 displays dramatically different kinetic behavior at higher pH values. At pH 5.1, SH-PTP1 shows apparent saturation kinetics with a K_M of 10.7 mM and a k_{cat} of 16.2 s^{-1}, comparable to those of SH-PTP1(ΔSH2) at this pH (Figure 3B). However, as pH increases its apparent K_M and k_{cat} values increase. At pH 5.4, the K_M and k_{cat} are 14.9 mM and 45.9 s^{-1}, respectively; at pH 5.7, these values increase to 86.8 mM and 80.4 s^{-1}; at pH 6.5, the V vs [S] plot becomes linear up to 35 mM pNPP, indicating a very large K_M value (>100 mM). SH-PTP1-(ΔC60), which lacks the entire C-terminal regulatory domain, shows qualitatively similar increases in the K_M value with pH (Figure 3C). Similar differences in kinetic behavior betweeen the two enzyme forms have also been observed with a pY peptide substrate (see below).

Activation of SH-PTP1 with pY Peptides. Our previous experiments with SH-PTP2, a similar SH2 domain-containing PTPase, demonstrated that occupancy of the SH2 domains with specific pY peptides stimulates its phosphatase activity by 10−50-fold (Lechleider et al., 1993b; Sugimoto et al., 1994). We asked whether pY peptides specific for the N-terminal SH2 domains of SH-PTP1 could activate SH-PTP1 in an analogous manner. We also anticipated using this activation as a quick means to screen for high-affinity ligands of the SH2 domains of SH-PTP1. As discussed above, SH-PTP1 has been reported to associate with tyrosyl phosphorylated c-Kit (Yi & Ihle, 1993), the IL-3 receptor β chain (Yi et al., 1993), and EPO receptor (U.X., U.L., L. C. Cantley, B.G.N., and H. F. Lodish, to be published elsewhere) via its N-terminal SH2 domain(s). For the EPOR/SH-PTP1 interaction, the SH-PTP1 binding site has been mapped to EPOR pY429. To test our hypothesis, 13 pY peptides corresponding to both known and potential phosphorylation sites on the above receptors as well as two other hematopoietic cell growth factor (cytokine) receptors were chemically synthesized and tested for their ability to activate SH-PTP1. These peptides include pY699 (GGVDpYKNIHLE), pY708 (LEKKpYVRRDSG), pY723 (VDTpYVEMRPVS), pY809 (NDSNpYIVKGNA), and pY969 (QPNNpYQFS) from the human CSF1 receptor (Coussens et al., 1986); pY355 (ASQVpYFTYDPYSE) of the IL-2 receptor β chain (Hataketama et al., 1989); pY936 (NHIpYSNLANSS), pY730 (GVSpYVVPTKAD), and pY747 (IGSpYIERDVTG) of human *c-kit* (Yarden et al., 1987); pY343 (AQDTpYLVLDK) and pY429 (Ac-PHLKpYLYLVVSDK) of the EPO receptor (D'Andrea et al., 1989); and pY628 (GSLEpYLCLPAGDK) and pY882 (KQQDpYLSLPPWE) of the IL-3 receptor β chain (Hayashida et al., 1990). SH-PTP1 activity was assayed at pH 7.4 with pNPP as substrate in the presence or absence of the above peptides. Addition of three peptides results in detectable activation of SH-PTP1 (Figure 4). The EPO receptor pY429 peptide, Ac-PHLKpYLYLVVSDK, is most effective, showing 28.6-fold stimulation of phosphatase activity at a concentration of 70 μM (Figure 4). At the same concentration, the corresponding unphosphorylated peptide (PHLKYLYLVVSDDDK; two additional aspartate residues were added to improve its solubility) shows a markedly reduced stimulatory effect of only 3.6-fold, consistent with the notion that activation is due to binding of this peptide to the SH2 domain(s). The IL-2Rβ pY355 peptide (ASQVpYFTYDPYSE) and the IL-3R pY628 peptide (GSLEpYLCLPAGDK) also result in 4.8- and 3-fold activation, respectively (at 70 μM). The unphosphorylated IL-3R peptide (GSLEYLCLPAGDK) has no effect. The other 10 pY peptides do not produce significant activation (<3-fold) (Figure 4 and data not shown).

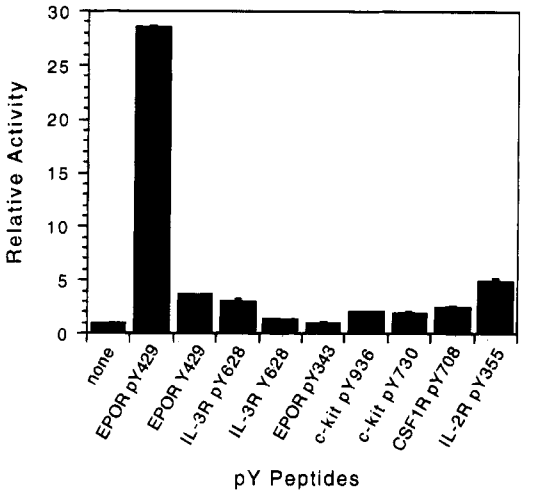

FIGURE 4: Effect of pY peptides on the catalytic activity of SH-PTP1 for pNPP hydrolysis. Dephosphorylation of pNPP (10 mM) was carried out in buffer A (pH 7.4) in the presence of 0 or 70 μM of the indicated pY peptides. Reactions were quenched with 1 N NaOH, and the amounts of pNPP hydrolyzed were determined by measuring the absorbances at 405 nm. The data presented are the mean ± SD values of initial rates from three parallel experiments, relative to those without pY peptide.

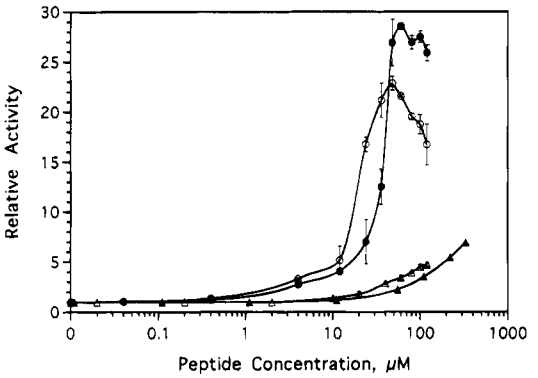

FIGURE 5: Concentration dependencies of activation of SH-PTP1 and R30K/R136K SH-PTP1. Closed circles, SH-PTP1 + EPOR pY429; open circles, R30K/R136K SH-PTP1 + EPOR pY429; open triangles, SH-PTP1 + EPOR Y429; and closed triangles, SH-PTP1 + IL-3R pY628. Experiments were carried out in buffer A (pH 7.4) with pNPP (10 mM) as substrate and in the presence of increasing amounts of the peptides. The data presented are the mean ± SD values of initial rates from three parallel experiments, relative to the basal activity of SH-PTP1.

Activation of SH-PTP1 by these pY peptides is concentration dependent (Figure 5). Below 1 μM there is very little stimulation. For the EPOR pY429 peptide, half-maximal activation occurs at approximately 40 μM and maximal activation of 25−30-fold is reached at 60−70 μM; higher concentrations result in greater inhibition, presumably via competition at the PTPase active site (see below). The nonphosphorylated Y429 peptide shows some stimulatory effect with 4.7-fold activation at 120 μM peptide, the highest concentration tested (higher concentrations are not possible due to insolubility). Activation by the IL-3R pY628 peptide is also much less effective as compared to the EPOR peptide.

Table 1: Leaving Group Dependence of SH-PTP1(ΔSH2)-Catalyzed Hydrolysis at pH 7.4, 23 °C

substrate	leaving group pK_a	K_M (mM)	k_{cat} (s^{-1})	k_{cat}/K_M (M^{-1} s^{-1})
pNPP	7.14	12.6	5.7	456
pCNPP	7.95	5.6	6.5	1150
mClPP	9.08	11.1	1.7	151
pFPP	9.95	10.2	1.6	159
PP	9.99	8.8	1.8	204
QPNNpYQFS	10.07	0.23	7.8	33913

Approximately 10-fold higher concentrations of the IL-3R pY628 peptide are required to achieve similar levels of activation, and maximal activation has not been reached at concentrations up to 330 μM (Figure 5). Therefore, all subsequent activation experiments were carried out with the EPOR pY429 peptide.

Catalytic Properties of SH-PTP1. The steady-state kinetics of the SH-PTP1(ΔSH2)-catalyzed hydrolysis of phenyl phosphate and four *para*- or *meta*-substituted derivatives were determined in order to examine the effect of leaving group pK_a on the k_{cat} values. Similar experiments with other PTPases have previously shown that their k_{cat} values display little dependence on the pK_a values of the various substituted phenyl leaving groups, suggesting that the hydrolysis of a common phosphoenzyme intermediate is the rate-limiting step (Zhang & Van Etten, 1991; Zhang et al., 1994). We carried out all hydrolysis reactions at pH 7.4, the same conditions as used for pY peptide activation studies. Table 1 lists the substrates, the pK_a values for their respective leaving groups, and the catalytic constants for each substrate. The k_{cat} values for these phenyl phosphate derivatives vary only 4-fold as the pK_a values of their leaving groups increase by almost 3 pH units. These data are consistent with breakdown of the phosphoenzyme intermediate as the rate-determining step along the catalytic pathway of SH-PTP1-(ΔSH2) at pH 7.4. The slight decrease in k_{cat} with increasing pK_a may suggest that, under these conditions, steps other than breakdown of the phosphoenzyme intermediate, most likely the formation of this intermediate, also begin to become partially rate-determining. We could not determine the leaving group dependence of full-length SH-PTP1-catalyzed reactions because SH-PTP1 does not exhibit saturation kinetics under the conditions.

Two dozen synthetic pY peptides derived from growth factor receptors, including the 13 pY peptides described above, have been tested as substrates of SH-PTP1 [also see Pei et al. (1993)]. All pY peptides are dephosphorylated by either wild-type SH-PTP1 or SH-PTP1(ΔSH2), albeit with varying efficiencies. Hydrolysis of one of these peptides, CSF1R pY969 (QPNNpYQFS), by SH-PTP1(ΔSH2) (at pH 7.4) shows saturation kinetics with a k_{cat} of 7.8 s^{-1}, a K_M of 230 μM, and a k_{cat}/K_M of 3.4×10^4 M^{-1} s^{-1} (Table 1). Under the same conditions, dephosphorylation of this peptide by full-length SH-PTP1 produces a straight line in its V vs [S] plot up to 1.4 mM peptide, with a k_{cat}/K_M of 490 M^{-1} s^{-1}. For the rest of these pY peptides, we have not been able to determine their kinetic constants with either enzyme form because the enzymes appear to have very low affinity toward these substrates (K_M > 2 mM). Two peptides with positively charged residues directly N-terminal to the pY, CSF1R pY708 (LEKKpYVRRDSG) and the activating EPOR pY429 (Ac-PHLKpYLYLVVSDK), are particularly poor substrates for SH-PTP1(ΔSH2). The V vs [S] plot for SH-PTP1-(ΔSH2)-catalyzed hydrolysis of EPOR pY429 peptide gives a straight line up to 200 μM peptide (a higher concentration was not possible due to limited solubility) and a k_{cat}/K_M value of only 450 M^{-1} s^{-1}. These data indicate that the presence of a positively charged residue directly N-terminal to the pY is disfavored by SH-PTP1. Indeed, a very similar peptide but with a glutamate instead of a lysine N-terminal to pY (Ac-GSLEpYLYLDLDK) shows markedly increased rate of hydrolysis by SH-PTP1(ΔSH2) (data not shown).

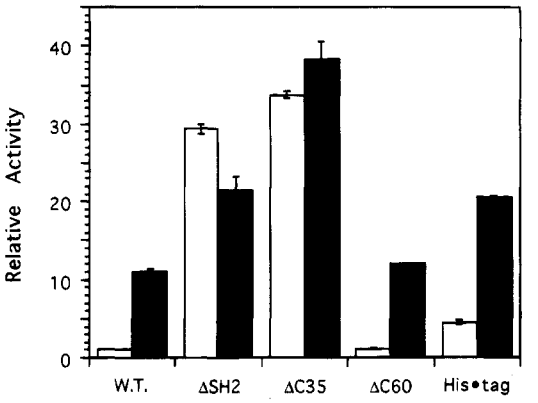

FIGURE 6: Activation of SH-PTP1 and mutants by EPOR pY429 peptide. Reactions were carried out with pNPP (10 mM) as substrate in buffer A (pH 7.4) in the absence (open bars) or presence (closed bars) of 60 μM EPOR pY429. The data presented are the mean ± SD values of relative initial rates (with respect to unstimulated wild-type SH-PTP1) from three independent experiments. These rates are normalized on a molar basis relative to wild-type SH-PTP1. The lower values of stimulated activities (11-fold vs 22−30-fold) observed here are most likely due to the small differences in the concentrations of the peptide used in the experiments and/or the different enzyme preparations.

Effect of Mutations and pH on Activation of SH-PTP1. The fully active SH-PTP1(ΔSH2) cannot be further stimulated by the EPOR pY429 peptide (at pH 7.4). Addition of 60 μM peptide results in approximately 25% inhibition of its phosphatase activity toward pNPP (down from 29-fold to 21.5-fold relative to SH-PTP1) (Figure 6). SH-PTP1-(ΔC35), which is already activated 34-fold by partial C-terminal truncation, is further stimulated by the peptide but to a much lesser extent (14% vs 11-fold for wild-type SH-PTP1). However, if one assumes that SH-PTP1(ΔC35) is also inhibited 25% by the pY peptide, then the net activation due to the pY peptide would be 39% relative to SH-PTP1(ΔC35) basal activity or 13-fold relative to SH-PTP1 basal activity. On the other hand, SH-PTP1(ΔC60) behaves much like wild-type SH-PTP1 showing a 12-fold stimulation upon treatment with EPOR pY429. SH-PTP1-(His•tag), in which a histidine tag (MGSSHHHHHHSS-GLVPRGSH) is added to the N-terminus of SH-PTP1, is stimulated by only 4.5-fold; however, because of its 4.5-fold higher basal activity, its specific activity after activation is 20.5-fold higher than SH-PTP1 basal activity, approaching that of SH-PTP1(ΔSH2).

Structural studies with the SH2 domains of Src, Abl, Lck, and SH-PTP2 have established that a universally conserved arginine residue at the βB5 position forms two hydrogen bonds with the negatively charged phosphate group of bound peptides (Overduin et al., 1992; Waksman et al., 1993; Eck et al., 1993; Lee et al., 1994). Mutation of this arginine to a lysine severely weakened the binding of Ab1 SH2 domain to pY ligands (Mayer et al., 1992). Similar R → K mutations in SH-PTP2 also resulted in partial loss of activation of the

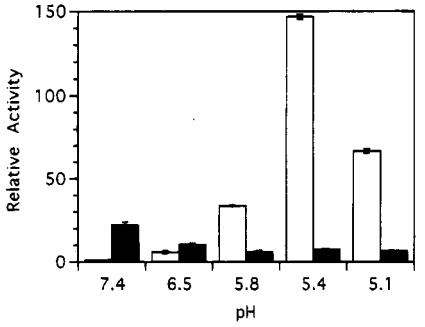

FIGURE 7: Effect of pH on activation of SH-PTP1 by the EPOR pY429 peptide. Reactions were carried out with pNPP (10 mM) as substrate at the indicated pH values in the absence (open bars) or presence (closed bars) of 70 μM pY peptide. The buffers used are described under Experimental Procedures. The data presented are the mean ± SD values of relative initial rates (with respect to unstimulated SH-PTP1 at pH 7.4) from three parallel experiments.

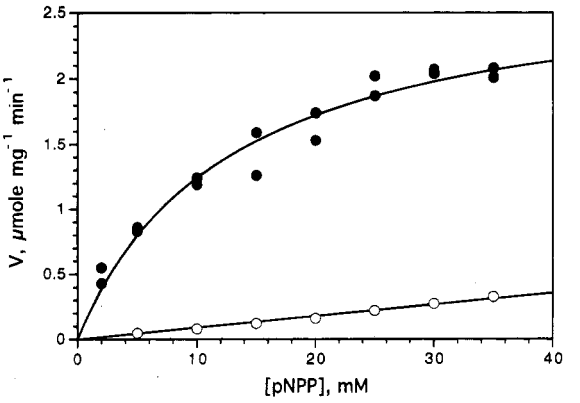

FIGURE 8: Effect of the EPOR pY429 peptide on the kinetic behavior of SH-PTP1 toward pNPP. Reactions were carried out at pH 7.4 (buffer A) with the indicated concentrations of pNPP in the absence (open circles) or presence (closed circle) of 40 μM EPOR pY429. The curves were fitted to the data (initial rates) according to the equation: $V = V_{max}[S]/(K_M + [S])$.

phosphatase by specific pY ligands (Sugimoto et al., 1994). In SH-PTP1, this conserved arginine is at positions 30 and 136 for the N- and C-terminal SH2 domains, respectively (Plutzky et al., 1992). We mutated both arginine residues to lysines and expected that the resulting R30K/R136K mutant would no longer bind the EPOR pY429 peptide. Surprisingly, this mutant can still be stimulated by the EPOR peptide, although the maximal activation is slightly lower (23-fold vs 28.6-fold for wild-type SH-PTP1) (Figure 5). Interestingly, activation of this mutant requires lower concentrations of EPOR pY429 peptide. Half-maximal activation is reached at 20 μM peptide (40 μM for wild-type SH-PTP1), and maximal activation is reached at 50 μM (60−70 μM for wild-type SH-PTP1).

The pH of the assay buffers greatly influences the ability of the EPOR pY429 peptide to activate SH-PTP1 (Figure 7). At pH 7.4, addition of 70 μM peptide typically results in 22−30-fold activation. At pH 6.5, this activation is less than 2-fold. At lower pH values (pH 5.8, 5.4, and 5.1), addition of 70 μM peptide actually results in 80−95% net inhibition of the phosphatase activity of SH-PTP1. The fully active SH-PTP1(ΔSH2) is inhibited by the peptide under all pH conditions (data not shown). These results are consistent with the notion that under acidic pH values, SH-PTP1 already exists in an active (open) conformation in the absence of pY peptides (see Discussion). Thus, addition of the EPOR pY429 peptide cannot further activate SH-PTP1 but instead results in competitive inhibition of the PTPase domain. It is also possible that the EPOR pY429 peptide has lower affinity for the SH2 domain(s) of SH-PTP1 under more acidic conditions. These two possibilities are not mutually exclusive.

Restoration of Saturation Kinetics of SH-PTP1 with EPOR Peptide. At neutral pH, SH-PTP1 displays nonsaturation kinetics. Its V vs [S] plot produces either a straight line or a sigmoidal curve, indicating the presence of allosteric activation by the substrates (pNPP and pY peptides) (Figures 3 and 8 and data not shown). However, when 40 μM EPOR pY429 peptide is added to the assay buffer (buffer A, pH 7.4), SH-PTP1 shows apparent saturation kinetics toward pNPP substrate with a K_M of 12.7 mM and a k_{cat} of 3.2 s^{-1} (Figure 8). These values are similar to those of SH-PTP1-(ΔSH2) under these conditions (K_M = 12.6 mM, k_{cat} = 5.7 s^{-1}), suggesting that addition of the EPOR pY429 peptide exerts an effect on SH-PTP1 similar to truncation of the two SH2 domains. Addition of higher concentrations of pY peptides to the assay buffer gives higher K_M values (for pNPP), probably because of increased competitive inhibition by the peptides (data not shown).

Binding of pY Peptides to SH-PTP1. Wild-type SH-PTP1 is not suitable for direct binding studies to pY peptides because hydrolysis of phosphotyrosyl residues by the catalytic domain would inevitably take place and the pY peptides would bind to the PTPase active site as well as the SH2 domains; both events would complicate quantitative analysis. Therefore, the isolated N-terminal or N+C-terminal SH2 domains were expressed as fusion proteins with maltose−binding protein, MBP-SH2(N) and MBP-SH2(N+C), respectively (Figure 1). We utilized MBP fusion proteins because the corresponding glutathione *S*-transferase fusion proteins are largely insoluble.

Binding experiments were conducted with a BIAcore biosensor, which uses surface plasmon resonance (SPR) to detect binding in real time (Malmqvist, 1993). The EPOR pY429 peptide (Ac-PHLKpYLYLVVSDK), with a lysine added to its C-terminus, was immobilized onto a (carboxymethyl)dextran polymer attached to a gold-coated surface within a flow chamber. Solutions containing SH2 proteins were passed over the surface, and the amount of protein associated with the immobilized peptide was determined by measuring the SPR signal (in RU). Under the conditions used, the amount of bound protein is directly proportional to the RU. Figure 9A displays the overlaid tracings from a set of BIAcore experiments. Injection of MBP-SH2(N) results in a rapid increase in RU due to the bulk solution. At the end of the injection the signal quickly drops followed by a delay phase due to the slow dissociation of bound SH2 molecules from the surface. The RU at the junction between the two phases (12 s after the end of injection) gives the amount of bound protein under equilibrium conditions. MBP protein alone up to 50 μM showed no binding to any of the peptides tested (data not shown). In addition, injection of free EPOR pY429 peptide during the slow phase was able to accelerate the release of bound SH2 proteins, presumably by preventing the released SH2 proteins from rebinding to the surface (data not shown). This suggests that the binding of SH2 protein to the surface is due to specific SH2-pY peptide association.

Solutions containing different amounts of SH2 proteins were passed through the BIAcore sensorchip, and the steady-

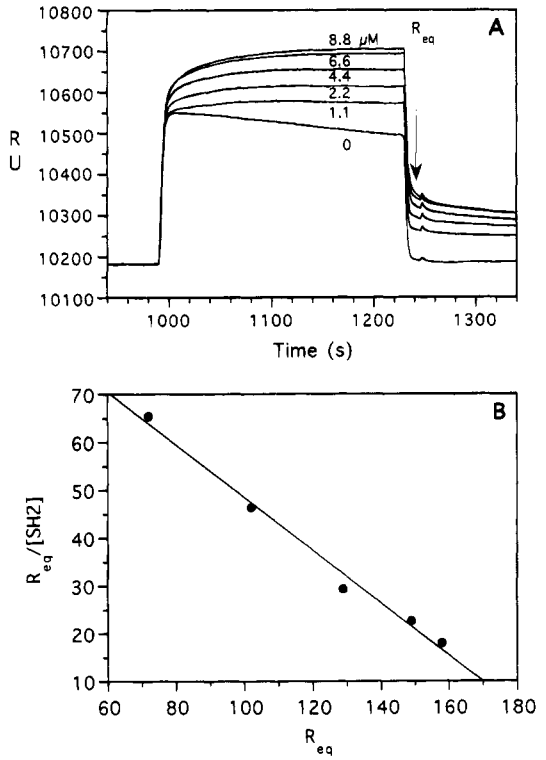

FIGURE 9: Binding of MBP-SH2(N) to the EPOR pY429 peptide. (A) Overlay of the BIAcore tracings from a set of experiments. Plotted is the resonance signal (RU) as a function of time. Various concentrations of MBP-SH2(N) (1.1, 2.2, 4.4, 6.6, and 8.8 μM) were passed over EPOR pY429 surface at a flow rate of 5 μL/min for 4 min. The R_{eq} data point used to determine K_D is indicated. (B) Scatchard analysis using the data from panel A.

state level of bound protein at each concentration was analyzed by Scatchard analysis. Figure 9B shows this analysis for the binding of MBP-SH2(N) to the EPOR pY429 peptide. The dissociation constant estimated by curve fitting for these data is 1.8 μM. MBP-SH2(N+C), which contains both SH2 domains of SH-PTP1 (Figure 1), shows reduced binding to the EPOR pY429 peptide. This decrease in binding is most likely a result of increased steric hindrance. We subsequently generated a construct of the isolated SH2-(N+C) domains (nonfusion, Figure 1). This protein binds the EPOR peptide with a K_D of 1.7 μM, similar to that of MBP-SH2(N). These results suggest that the N-terminal SH2 domain is primarily responsible for the binding observed. MBP-SH2(N+C/R30K/R136K), in which the two arginine residues (R30 and R136) expected to contact the phosphate group in an SH2-pY complex have been mutated to lysines, still shows detectable binding to the EPOR pY peptide, although the amount of binding is decreased (~2-fold) compared to MBP-SH2(N+C) (data not shown). Due to the limited solubility of EPOR Y429 peptide (nonphosphorylated) and lack of a convenient method to monitor its loading on sensorchips, we have not been able to directly test the binding of this peptide to SH-PTP1 SH2 domains. However, we have observed that when the immobilized EPOR pY429 peptide loses its phosphate group (as monitored by anti-pY antibody) over the course of our experiments, the amount of binding by the SH2 domains drops accordingly. This indicates that the phosphate group is essential for SH2 binding.

In order to determine whether the EPOR pY429 peptide also binds the catalytic domain of SH-PTP1, we mutated the conserved catalytic residue, cysteine 453, to a serine. The C453S mutant is inactive and could be used for binding pY peptides on a BIAcore instrument. SH-PTP1(ΔSH2/C453S) binds strongly to the sensorchip derivatized with the EPOR pY peptide. However, when the positively charged C-terminus was removed, which had contributed to the binding to the negatively charged (carboxymethyl)dextran surface, the resulting catalytic core, SH-PTP1(ΔSH2/ΔC60/C453S), shows no significant binding to the immobilized EPOR pY429 peptide.

Seven other pY peptides (CSF1R pY969, Il-2R pY355, c-Kit pY936, pY930, and pY747, EPOR pY343, and IL-3R pY628) were also immobilized onto sensorchips and tested for binding to MBP-SH2(N). The IL-3R pY628 peptide gives a significant binding signal, but the binding is too weak to allow accurate measurements of its K_D on the BIAcore instrument under the conditions used in this work. We estimate that its dissociation constant is 4−10 μM. The rest of the pY peptides do not show significant binding. We have not tested whether the C-terminal SH2 domain of SH-PTP1 binds these pY peptides. It is conceivable that the IL-2R pY355 peptide activates SH-PTP1 by binding to its C-terminal SH2 domain.

DISCUSSION

In this work, we have provided kinetic evidence for autoinhibition of a protein tyrosine phosphatase via an intramolecular phosphotyrosine-independent interaction with its own SH2 domain(s). This autoinhibition can be relieved by pY ligand binding to the SH2 domains.

Recombinant SH-PTP1 and SH-PTP1(ΔSH2), which contain the identical catalytic domain, display distinct kinetic behavior. Although both enzymes show strong pH dependence, they have different pH profiles; SH-PTP1 is most active at pH 5.5, whereas SH-PTP1(ΔSH2) is most active at pH 6.3 (Pei et al., 1993). Over a range of substrate concentrations tested, SH-PTP1(ΔSH2) is significantly more active than SH-PTP1. For example, the truncation mutant is 30-fold more active at physiological pH (7.4). This indicates that the SH2 domains play a direct regulatory role in attenuating the activity of SH-PTP1.

Steady-state kinetic studies at various pH values reveal that for SH-PTP1(ΔSH2), its pH dependence derives mostly from changes in k_{cat} values, since its K_M value is essentially unchanged (10−14 mM) over a range of pH (5.1−7.4). The similar k_{cat} values for SH-PTP1(ΔSH2)-catalyzed hydrolysis of five phenyl phosphate derivatives suggest that the breakdown of the phosphoenzyme intermediate is the rate-limiting step. For SH-PTP1, however, its K_M value increases dramatically with pH and, at pH 7.4, is much higher than that of SH-PTP1(ΔSH2). Recently, Townley et al. (1993) also reported a 22−25-fold decrease in K_M toward a triphosphorylated insulin receptor peptide substrate when either the N-terminal or both SH2 domains were removed, whereas the k_{cat} value remained largely unchanged. Thus, the distinct pH profile and the reduced catalytic activity of SH-PTP1 relative to SH-PTP1(ΔSH2) must be due, at least in part, to impaired binding of substrates to the PTPase active site in SH-PTP1.

How can the SH2 domains affect the binding of substrates to the PTPase active site? Here we propose a model in which the N-terminal SH2 domain (and possibly the C-terminal SH2 domain as well) directly interacts with the PTPase domain or the C-terminus in a reversible, noncovalent fashion

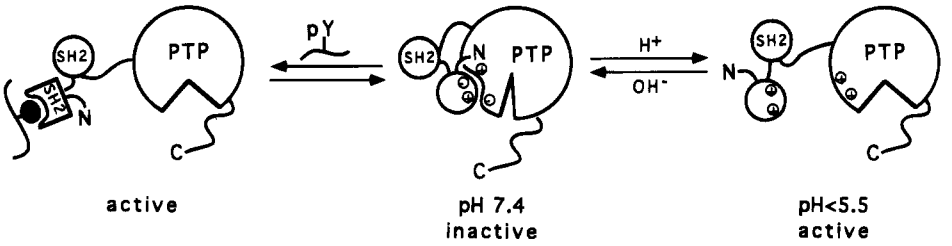

FIGURE 10: Model showing autoregulation of SH-PTP1 by its SH2 domains. In the middle part of the figure, at neutral pH, SH-PTP1 is negatively autoregulated by interaction of the N-terminal SH2 domain with the PTPase catalytic domain (in the absence of a specific pY ligand for the C-terminal SH2 domain; its role is not yet clear). This inhibition can be overcome either by titration of one or more residues to their conjugated acid forms at pH ≤ 5.5 (right-hand side) or by engagement of the N-terminal SH2 by a specific pY ligand (left-hand side).

(Figure 10). Since SH-PTP1(ΔC60), which lacks essentially the entire C-terminus, behaves similarly to SH-PTP1 in pH-dependent kinetics and activation by the EPOR pY429 peptide, it seems unlikely that the SH2 domain-interacting site resides on the C-terminus. Furthermore, this interaction appears to be intramolecular, since SH-PTP1 exists apparently as monomers under these conditions (Pei et al., 1993). Presumably, the SH2 domain−PTPase domain interaction involves a key ion pair(s), which is(are) titrated at a pH of approximately 5.5. Above pH 5.5, the SH2 domain−PTPase domain interaction perhaps physically blocks the access of substrate to the PTPase active site and/or changes its active site conformation, rendering the PTPase inactive (closed state); at pH < 5.5, SH2 domain−PTPase domain interactions might be disrupted by the loss of the ion pair(s), freeing the PTPase domain, which then relaxes back to its active conformation (open state). Consistent with this model, the pH profiles show that at pH > 5.5, SH-PTP1(ΔSH2) is consistently more active than SH-PTP1, whereas at pH < 5.5, the activity of SH-PTP1 approaches that of SH-PTP1-(ΔSH2) (Pei et al., 1993). Also consistent with the model, addition of a histidine tag (MGSSHHHHHHSSGLVPRGSH) to the N-terminus of SH-PTP1 activates the enzyme [SH-PTP1(His•tag)] by 4.5-fold, perhaps because the tag interferes with the intramolecular interdomain interactions. Alternatively, at pH 7.4, the seven histidines and the arginine in the tag would be partially positively charged, and these charges might disengage the ion pair(s) essential for the interdomain interactions. A third line of evidence comes from a recent report by Dechert et al. (1994) that the isolated SH2 domains of SH-PTP2, which is highly similar to SH-PTP1, can physically associate with the PTPase domain and inhibit the catalytic activity of SH-PTP2 in a concentration-dependent manner. We have independently carried out a similar experiment with SH-PTP1. However, we did not observe significant association between the SH2 domains and the PTPase domain. This could be due to the lower affinity between the two domains in SH-PTP1 as compared to SH-PTP2 (see below).

The above model explains the pH-dependent behavior of SH-PTP1. At pH 5.1 and 5.4, SH-PTP1 would exist in an open state and thus behave much like SH-PTP1(ΔSH2), displaying saturation kinetics (Figure 3B). Indeed, at pH 5.1, the kinetic parameters for full-length SH-PTP1 (K_M = 10.7 mM, k_{cat} = 16.2 s^{-1}, and k_{cat}/K_M = 1.5 × 10^3 M^{-1} s^{-1}) and SH-PTP1(ΔSH2) (K_M = 12.8 mM, k_{cat} = 12.2 s^{-1}, and k_{cat}/K_M = 1.0 × 10^3 M^{-1} s^{-1}) are comparable. At higher pH, for example pH 5.7 or 6.5, SH-PTP1 would adopt a closed conformation (Figure 10). pNPP or pY peptide substrates would bind to the SH2 domain(s) as well as to the PTPase active site. Occupancy of the SH2 domain(s) could induce a conformational change, which could interfere with the interdomain interactions and drive SH-PTP1 to the open conformation, resulting in elevated catalytic activity. Since higher concentrations of substrate would shift the equilibrium further toward the open conformation, the V vs [S] plot reflects a linear titration of SH-PTP1 away from the closed conformation (Figure 10). The dramatic lowering of K_M for pNPP (at the same k_{cat}) either by truncation of the SH2 domains or upon binding of a phosphotyrosine ligand is consistent with increasing the number of active enzyme molecules. Conformational change of SH2 domains induced upon binding to phosphotyrosyl peptides has previously been demonstrated with the N-terminal SH2 domain in the p85 subunit of phosphatidylinositol 3-kinase (Panayotou et al., 1992; Shoelson et al., 1993). Dechert et al. (1994) also observed that a PDGFR pY peptide is able to eliminate the intermolecular association between the isolated SH2 domains and the PTPase domain of SH-PTP2.

The presence of SH2 domains in SH-PTP1, SH-PTP2, and *corkscrew* implies that these PTPases may be involved in signal transduction pathways via binding to specific sites of tyrosyl-phosphorylated proteins, such as growth factor receptors. Indeed, SH-PTP2 has been shown to associate with the activated PDGF receptor (Feng et al., 1993; Vogel et al., 1993; Lechleider et al., 1993a), EGF receptor (Vogel et al., 1993; Lechleider et al., 1993a), and insulin receptor substrate 1 (Kuhne et al., 1993). SH-PTP1 has been reported to associate with *c-kit* (Yi & Ihle, 1993), the IL-3 receptor β chain (Yi et al., 1993), and EPO receptor pY429 (U.X., U.L., L. C. Cantley, B.G.N., and H. F. Lodish, to be published elsewhere). SH-PTP1 also undergoes phosphorylation on serine residues and at tyrosine 564 in activated T cell lines (Lorenz et al., 1994) and on as-yet-unidentified tyrosine residues upon CSF-1 stimulation of a macrophage cell line (Yeung et al., 1992; Yi & Ihle, 1993) or primary murine macrophages (S. Chang, U.L., and B.G.N., unpublished results). Because of its essential role during hematopoiesis (Shultz et al., 1993), it has been hypothesized that SH-PTP1 may play a key regulatory role in signaling through the IL-3 receptor in leukocytes (Yi et al., 1993) and the EPO receptor in erythroid cells (U.X., U.L., L. C. Cantley, B.G.N., and H. F. Lodish, to be published elsewhere). We thus tested a variety of synthetic pY peptides corresponding to known and potential phosphorylation sites in several hematopoietic cell receptors for their ability to bind and activate SH-PTP1. Among them, EPOR pY429, IL-3R pY628, and IL-2Rβ pY355 peptides result in significant activation of SH-PTP1 in a concentration-dependent manner (28.6-, 3-, and 4.8-fold, respectively, at 70 μM). The corresponding nonphospho-

peptides are much less efficient in activating SH-PTP1, consistent with the model that these pY peptides activate SH-PTP1 by binding to its N-terminal SH2 domain(s). An alternative explanation may be that the pY peptides compete with the SH2 domain(s) for the PTPase active site, forcing it into an open (active) conformation. However, this seems unlikely, since the EPOR pY429 peptide does not bind the PTPase domain during BIAcore assays. Furthermore, CSF-1R pY969 peptide (QPNNpYQFS), which is a much better substrate for SH-PTP1 than either of the above three peptides, fails to achieve significant activation of SH-PTP1.

The isolated N-terminal SH2 domain of SH-PTP1 (as MBP fusion protein) binds the EPOR pY429 peptide with a dissociation constant of 1.8 μM. The IL-3R pY628 peptide has a 2−6-fold lower affinity for MBP-SH2(N). If one takes into account the greater inhibition by the IL-3R pY628 peptide (it is a much better substrate than the EPOR pY429 peptide for the PTPase domain), this correlates well with the observation that a ~10-fold higher concentration of the IL-3Rβ pY628 peptide is required to achieve the same level of activation of SH-PTP1 as EPOR pY429 (Figure 5). These results also suggest that pY628 may be the *in vivo* binding site on the IL-3 receptor for SH-PTP1, although additional site(s) on the receptor may also be important for high-affinity association. One point worth mentioning is that the above K_D values are 1−3 orders of magnitude higher than those reported for pY peptides binding to other SH2 domains, such as those of Src (Payne et al., 1993; Bibbins et al., 1993), Lck (Payne et al., 1993), PI3 kinase (Felder et al., 1993), and SH-PTP2 (Sugimoto et al., 1994). We believe that pY peptides with higher affinity to SH-PTP1 SH2 domains might yet be discovered. A surprising result is that R30K/R136K SH-PTP1 with its two conserved pY-binding arginines mutated can still bind to and be stimulated by the EPOR pY429 peptide. Further experimentation is necessary to understand this phenomenon. Bibbins et al. (1993) have previously reported that a R175L mutant of Src SH2 domain is still capable of high-affinity binding to a PDGFR pY751 peptide.

Half-maximal activation of SH-PTP1 is achieved at 40 μM with the EPOR pY429 peptide, a value 20-fold higher than the dissociation constant of the isolated SH2 domain for this peptide ($K_D \sim 1.8$ μM). A possible explanation is that in full-length SH-PTP1 extra energy must be expended to disrupt the SH2 domain−PTPase domain interactions before the peptide can bind the SH2 domain(s). A similar phenomenon has also been observed with SH-PTP2, for which an even larger excess (1000-fold) of specific pY peptides is required to achieve half-maximal activation (Lechleider et al., 1993b; Sugimoto et al., 1994). This may suggest that the affinity between the SH2 domains and the PTPase domain is higher in SH-PTP2 than in SH-PTP1. Consistent with this view, R30K/R136K SH-PTP1, in which the mutations have presumably weakened the interdomain association somewhat, shows an earlier half-maximal activation (at 20 μM peptide).

Maximally activated SH-PTP1 (at 70 μM EPOR pY429 peptide) is 25−30-fold more active than unactivated SH-PTP1 (basal activity). Under the same conditions SH-PTP1-(ΔSH2) is 30-fold more active in the absence of the peptide; the addition of 60 μM EPOR pY429 peptide inhibits its activity by 25%, down to 21.5-fold relative to the basal activity. This suggests that in the presence of 70 μM peptide the vast majority of SH-PTP1 is in the open (active) state, as in SH-PTP1(ΔSH2). Indeed, addition of 40 μM EPOR pY429 peptide results in a switch from nonsaturation to saturation kinetic behavior of SH-PTP1 toward pNPP at pH 7.4, with catalytic parameters ($k_{cat} = 3.2$ s^{-1}, $K_M = 12.7$ mM) similar to those of SH-PTP1(ΔSH2) ($k_{cat} = 5.7$ s^{-1}, $K_M = 12.6$ mM).

The extended C-terminus can also exert a modulatory role. Truncation of the last 35 amino acids activates the enzyme [SH-PTP1(ΔC35)] by 20−34-fold with either pNPP, pY peptides, or RCM-lysozyme as substrate (at pH 7.4). Zhao et al. (1993) previously reported that removal of the last 41 amino acids by trypsin treatment also resulted in a 20-fold activation toward RCM-lysozyme but not toward pNPP. We believe that the different results observed with pNPP are most likely due to the pH difference of the assay buffers (Zhao et al. carried out pNPP assays at pH 5.0). At pH 5.1, we did not observe significant activation with either substrate. Interestingly, SH-PTP1(ΔC35) is only marginally stimulated by the EPOR pY429 peptide (14%). However, when one extends the truncation to the C-terminal 60 amino acids, the resulting enzyme behaves like wild-type SH-PTP1, including stimulation with pY peptides. It appears that the partial C-terminal truncation exposes some sequence elements resident within the N-terminal half of the C-terminus (amino acids 536−560), which can activate the PTPase domain by increasing the rate of one or more of the steps prior to breakdown of the covalent phosphoenzyme intermediate. Binding of specific pY ligands appears to have a similar effect. Presumably, the increase in the rate(s) of this step-(s), which was kinetically limiting, shifts the rate-limiting step along the PTPase catalytic pathway to the hydrolysis of the phosphocysteinyl enzyme intermediate, as in SH-PTP1(ΔSH2) (Guan & Dixon, 1991; Zhang & Van Etten, 1991; Cho et al., 1992; Zhang et al., 1994). It is not yet clear whether proteolytic cleavage of the C-terminus occurs *in vivo*. However, other posttranslational modifications (e.g., phosphorylation) and/or association with partner proteins could have a similar effect. In this regard, it is particularly interesting to note that the two known tyrosine phosphorylation sites (pY536 and pY564) reside in this part of the C-terminus (Lorenz et al., 1994). Indeed, phosphorylation of Y536 has been reported to activate SH-PTP1 3−4-fold (Uchida et al., 1994). Whether the SH2 domains and the C-terminus [e.g., pY forms interacting with SH2 domain-(s)] act in concert in regulating the catalytic domain remains to be determined.

In conclusion, kinetic analysis of SH-PTP1 and mutants has revealed a negative regulatory function of the SH2 domains. This regulation is most likely due to an intramolecular interaction between the SH2 domain(s) and the catalytic domain. Because proteins purified from *E. coli* are presumably free of tyrosine phosphorylation, and because SH-PTP1(ΔC60), which lacks the known *in vivo* and *in vitro* tyrosyl phosphorylation sites (Lorenz et al., 1994), still displays the SH2 domain-mediated autoregulation, the SH2 domain-PTPase domain interactions must be phosphotyrosine independent. This basal inhibition can be relieved as pY ligands compete with the catalytic domain for binding to the SH2 domains and thereby activate PTPase activity by an order of magnitude for both SH-PTP1 and SH-PTP2. We are currently conducting experiments to identify the sites of interaction between SH2 domains and the catalytic domain.

ACKNOWLEDGMENT

We thank T. Wandless and M. Lamarche for the preparation of radiolabeled RCM-lysozyme and the phenyl phosphate derivatives, E. Lyszak for construction and purification of SH-PTP1(ΔSH2/ΔC60/C453S) mutant, and Jim Lee for mass spectrometry analysis of the synthetic peptides. We would also like to thank J. M. Bollinger, L. Stolz, P. Cole, and T. Wandless for critical reading of this manuscript.

REFERENCES

Ahmad, S., Banville, D., Zhao, Z., Fischer, E. H., & Shen, S.-H. (1993) *Proc. Natl. Acad. Sci. U.S.A. 90*, 2197−2201.

Bibbins, K. B., Boeuf, H., & Varmus, H. E. (1993) *Mol. Cell. Biol. 13*, 7278−7287.

Bradford, M. M. (1976) *Anal. Biochem. 72*, 248−254.

Cho, H., Ramer, S. E., Itoh, M., Winkler, D. G., Kitas, E., Bannwarth, W., Burn, P., Saito, H., & Walsh, C. T. (1991) *Biochemistry 30*, 6210−6216.

Cho, H., Krishnaraj, R., Kitas, E., Bannwarth, W., Walsh, C. T., & Anderson, K. S. (1992) *J. Am. Chem. Soc. 114*, 7296−7298.

Coussens, L., Beveren, C. V., Smith, D., Chen, E., Mitchell, R. L., Isacke, C. M., Verma, I. M., & Ullrich, A. (1986) *Nature 320*, 277−280.

D'Andrea, A. D., Lodish, H. F., & Wong, G. G. (1989) *Cell 57*, 277−285.

Dechert, U., Adam, M., Harder, K. W., Clark-Lewis, I., & Jirik, F. (1994) *J. Biol. Chem. 269*, 5602−5611.

Eck, M., Shoelson, S. E., & Harrison, S. C. (1993) *Nature 362*, 87−91.

Felder, S., Zhou, M., Hu, P., Urena, J., Ullrich, A., Chaudhuri, M., White, M., Shoelson, S. E., & Schlessinger, J. (1993) *Mol. Cell. Biol. 13*, 1449−1455.

Feng, G.-S., Hui, C. C., & Pawson, T. (1993) *Science 259*, 1607−1611.

Fischer, E. H., Charbonneau, H., & Tonks, N. K. (1991) *Science 253*, 401−406.

Freeman, R. M., Jr., Plutzky, J., & Neel, B. G. (1992) *Proc. Natl. Acad. Sci. U.S.A. 89*, 11239−11243.

Guan, K. L., & Dixon, J. E. (1991) *J. Biol. Chem. 266*, 17026−17030.

Hatakeyama, M., Tsudo, M., Minamoto, S., Kono, T., Doi, T., Miyata, T., Miyasaka, M., & Taniguchi, T. (1989) *Science 244*, 551−556.

Hayashida, K., Kitamura, T., Gorman, D. M., Arai, K., Yokota, T., & Miyajima, A. (1990) *Proc. Natl. Acad. Sci. U.S.A. 87*, 9655−9659.

Kazlauskas, A., Feng, G.-S., Pawson, T., & Valius, M. (1993) *Proc. Natl. Acad. Sci. U.S.A. 90*, 6939−6942.

Kitas, E. A., Perich, J. W., Wade, J. D., Johns, R. B., & Tregear, G. W. (1989) *Tetrahedron Lett. 30*, 6229−6232.

Koch, C. A., Anderson, D., Moran, M. F., Ellis, C., & Pawson, T. (1991) *Science 252*, 668−674.

Kuhne, M. R., Pawson, T., Lienhard, G. E., Feng, G.-S. (1993) *J. Biol. Chem. 268*, 11479−11481.

Kunkel, T. A. (1985) *Proc. Natl. Acad. Sci. U.S.A. 82*, 488−492.

Lechleider, R. J., Freeman, R. M., Jr., & Neel, B. G. (1993a) *J. Biol. Chem. 268*, 13434−13438.

Lechleider, R. J., Sugimoto, S., Bennett, A. M., Kashishian, A. S., Cooper, J., Shoelson, S. E., Walsh, C. T., & Neel, B. G. (1993b) *J. Biol. Chem. 268*, 21478−21481.

Lee, C.-H., Kominos, D., Jacques, S., Margolis, B., Schlessinger, J., Shoelson, S. E., & Kuriyan, J. (1994) *Structure 2*, 423−438.

Lorenz, U., Ravichandran, K. S., Pei, D., Walsh, C. T., Burakoff, S. J., & Neel, B. G. (1994) *Mol. Cell. Biol. 14*, 1824−1834.

Malmqvist, M. (1993) *Nature 361*, 186−187.

Matthews, R. J., Bowne, D. B., Flores, E., & Thomas, M. L. (1992) *Mol. Cell. Biol. 12*, 2396−2405.

Mayer, B. J., Jackson, P. K., Van Etten, R. A., & Baltimore, D. (1992) *Mol. Cell. Biol. 12*, 609−618.

Overduin, M., Rios, C. B., Mayer, B. J., Baltimore, D., & Cowburn, D. (1992) *Cell 70*, 697−704.

Panayotou, G., Bax, B., Gout, I., Federwisch, M., Wroblowski, B., Dhand, R., Fry, M. J., Blundell, T. L., Wollmer, A., & Waterfield, M. D. (1992) *EMBO J. 11*, 4261−4272.

Payne, G., Shoelson, S. E., Gish, G. D., Pawson, T., & Walsh, C. T. (1993) *Proc. Natl. Acad. Sci. U.S.A. 90*, 4902−4906.

Pei, D., Neel, B. G., & Walsh, C. T. (1993) *Proc. Natl. Acad. Sci. U.S.A. 90*, 1092−1096.

Perkins, L. A., Larsen, I., & Perrimon, N. (1992) *Cell 70*, 225−236.

Plutzky, J., Neel, B. G., & Rosenberg, R. D. (1992) *Proc. Natl. Acad. Sci. U.S.A. 89*, 1123−1127.

Riggs, P. (1990) in *Current Protocols in Molecular Biology* (Ausebel, et al., Eds.) pp 16.0.1−16.6.12, Greene Associates/Wiley Interscience, New York.

Shen, S.-H., Bastien, L., Posner, B. I., & Chretien, P. (1991) *Nature 352*, 736−739.

Shoelson, S. E., Sivaraja, M., Williams, K. P., Hu, P., Schlessinger, J., & Weiss, M. A. (1993) *EMBO J. 12*, 795−802.

Shultz, L. D., Schweitzer, P. A., Rajan, T. V., Yi, T., Ihle, J. N., Matthews, R. J., Thomas, M. L., & Beier, D. R. (1993) *Cell 73*, 1445−1454.

Songyang, Z., Shoelson, S. E., Chaudhuri, M., Gish, G., Pawson, T., Haser, W. G., King, F., Roberts, T., Ratnofsky, S., Leachleider, R. J., Neel, B. G., Brige, R. B., Fajardo, J. E., Chou, M. M., Hanafusa, H., Schhausen, B., & Cantley, L. C. (1993) *Cell 72*, 767−778.

Sugimoto, S., Lechleider, R. J., Shoelson, S. E., Neel, B. G., & Walsh, C. T. (1993) *J. Biol. Chem. 268*, 22771−22776.

Sugimoto, S., Wandless, T. J., Shoelson, S. E., Neel, B. G., & Walsh, C. T. (1994) *J. Biol. Chem. 269*, 13614−13622.

Sun, X. J., Crimmins, D. L., Myers, M. G., Miralpeix, M., & White, M. F. (1993) *Mol. Cell. Biol. 13*, 7418−7428.

Townley, R., Shen, S.-H., Banville, D., & Ramanchandran, C. (1993) *Biochemistry 32*, 13414−13418.

Uchida, T., Matozaki, T., Noguchi, T., Yamao, T., Horita, K., Suzuki, T., Fujioka, Y., Sakamoto, C., & Kasuga, M. (1994) *J. Biol. Chem. 269*, 12220−12228.

Vogel, W., Lammers, R., Huang, J., & Ullrich, A. (1993) *Science 259*, 1611−1614.

Waksman, G., Shoelson, S. E., Pant, N., Cowburn, D., & Kuriyan, J. (1993) *Cell 72*, 779−790.

Yarden, K., Kuang, W.-J., Yang-Feng, T., Coussens, L., Munemitsu, S., Dull, T. J., Chen, E., Schlessinger, J., Francke, V., & Ullrich, A. (1987) *EMBO J. 6*, 3341−3351.

Yeung, Y.-G., Berg, K. L., Pixley, F. J., Angeletti, R. H., & Stanley, E. R. (1992) *J. Biol. Chem. 267*, 23447−23450.

Yi, T., & Ihle, J. N. (1993) *Mol. Cell. Biol. 13*, 3350−3358.

Yi, T., Cleveland, J. L., & Ihle, J. N. (1992) *Mol. Cell. Biol. 12*, 836−846.

Yi, T., Mui, A. L. F., Krystal, G., & Ihle, J. N. (1993) *Mol. Cell. Biol. 13*, 7577−7586.

Zhang, Z.-Y., & Van Etten, R. L. (1991) *J. Biol. Chem. 266*, 1516−1525.

Zhang, Z.-Y., Malachowski, W. P., Van Etten, R. L., & Dixon, J. E. (1994) *J. Biol. Chem. 269*, 8140−8145.

Zhao, Z., Bouchard, P., Diltz, C. D., Shen, S.-H., & Fischer, E. H. (1993) *J. Biol. Chem. 268*, 2816−2820.

BI942257D